Simulations of Localized States of Stationary Convection in ^{3}He-^{4}He Mixtures

Oriol Batiste[1] and Edgar Knobloch[2]

[1]*Departament de Física Aplicada, Universitat Politècnica de Catalunya, Barcelona, Spain*
[2]*Department of Physics, University of California, Berkeley, California 94720, USA*

(Received 14 January 2005; published 5 December 2005)

Simulations of convection in ^{3}He-^{4}He mixtures with a negative separation ratio in two-dimensional containers with realistic boundary conditions and moderately large aspect ratio reveal, at supercritical Rayleigh numbers, the existence of "convectons," i.e., localized states of stationary convection, separated by regions of no convection. The origin and properties of these states are described.

DOI: 10.1103/PhysRevLett.95.244501 PACS numbers: 47.20.Bp, 47.20.Ky, 47.27.Te, 47.54.+r

Binary fluid mixtures with a negative separation ratio exhibit a wide variety of behavior when heated from below. Of particular interest are traveling wave states with complex time-dependence present very close to the onset of the initial instability [1–3], some spatially extended [4] and others localized [5]. Experiments on water-ethanol mixtures in annular containers have also revealed the presence of dispersive chaos [6,7], as well as localized states of steady convection apparently stabilized by incident traveling waves [7,8]. In this *Letter* we report on a novel state, resembling the latter state, but comprising of one (or more) localized states consisting of steady convection rolls separated by regions of no motion: regions in which flow, whether in the form of weak convection or spatially growing traveling waves, is entirely absent, despite spatially uniform heating from below. In the following we refer to these states as *convectons* [9].

Binary mixtures are characterized by cross diffusion quantified by the separation ratio S. When $S < 0$ the heavier component (of concentration C) migrates up the temperature gradient. Thus in a layer heated from below the destabilizing temperature gradient competes with a stabilizing concentration gradient that develops in response to the heating. If this effect is strong enough convection sets in as growing oscillations once the Rayleigh number R exceeds a critical value R_c; this instability is typically subcritical and develops into a variety of traveling wave states depending on parameters and initial conditions. Once $\epsilon \equiv (R - R_c)/R_c \gtrsim \Gamma^{-2}$, where $\Gamma \gg 1$ is the container aspect ratio, the waves may become spatially localized [10] indicating a transition to behavior characteristic of extended systems [11]. Within this regime we have found spatially localized *steady* convection. In the following we describe the origin of this state and its properties.

Our calculations are performed for parameters characteristic of ^{3}He-^{4}He mixtures [1,12,13] with no-slip boundary conditions at the top and bottom, and on the sidewalls if present. The temperature is imposed at top ($T = T_0$) and bottom ($T = T_1$) and the mass flux vanishes on all walls. The system is then described by the equations [14]

$$\mathbf{u}_t + (\mathbf{u}\cdot\nabla)\mathbf{u} = -\nabla P + \sigma R[(1+S)\theta - S\eta]\hat{\mathbf{z}} + \sigma\nabla^2\mathbf{u}, \tag{1}$$

$$\theta_t + (\mathbf{u}\cdot\nabla)\theta = w + \nabla^2\theta, \tag{2}$$

$$\eta_t + (\mathbf{u}\cdot\nabla)\eta = \tau\nabla^2\eta + \nabla^2\theta, \tag{3}$$

together with the incompressibility condition

$$\nabla\cdot\mathbf{u} = 0. \tag{4}$$

Here $\mathbf{u} \equiv (u, w)$ is the velocity field in (x, z) coordinates, P is the pressure, and θ denotes the departure of the temperature from its conduction profile, in units of the imposed temperature difference $\Delta T = T_1 - T_0 > 0$. The variable η is defined such that its gradient represents the dimensionless convective mass flux. Thus $\eta \equiv \theta - \Sigma$, where $C = 1 - z + \Sigma$ is the concentration of the heavier component in units of the concentration difference that develops across the layer as a result of cross diffusion. The system is specified by four dimensionless parameters: the Rayleigh number R providing a dimensionless measure of the imposed temperature difference ΔT, the separation ratio S that measures the resulting concentration contribution to the buoyancy force due to cross diffusion, and the Prandtl and Lewis numbers σ, τ, in addition to the aspect ratio Γ. The boundary conditions are $\mathbf{u} = \theta = \eta_z = 0$ on $z = 0, 1$, with either periodic boundary conditions in the horizontal with period Γ, or $\mathbf{u} = \theta_x = \eta_x = 0$ on $x = 0, \Gamma$.

In Fig. 1 we show two *coexisting* convectons computed with periodic boundary conditions when $R = 2800$, $\Gamma = 20$. Figure 1(a) shows an odd parity convecton, while Fig. 1(b) is of even parity; both are time independent and numerically stable. Each state is described in terms of the contours of the temperature fluctuation $\theta(x, z)$ and of the associated concentration $C(x, z)$. In addition, the lowest panel shows the concentration at $z = 1/2$. Both states consist of steady rolls, separated by two fronts from a convection-free region. Since concentration gradients are expelled from regions of closed streamlines the rolls are well mixed, with large concentration gradients along the

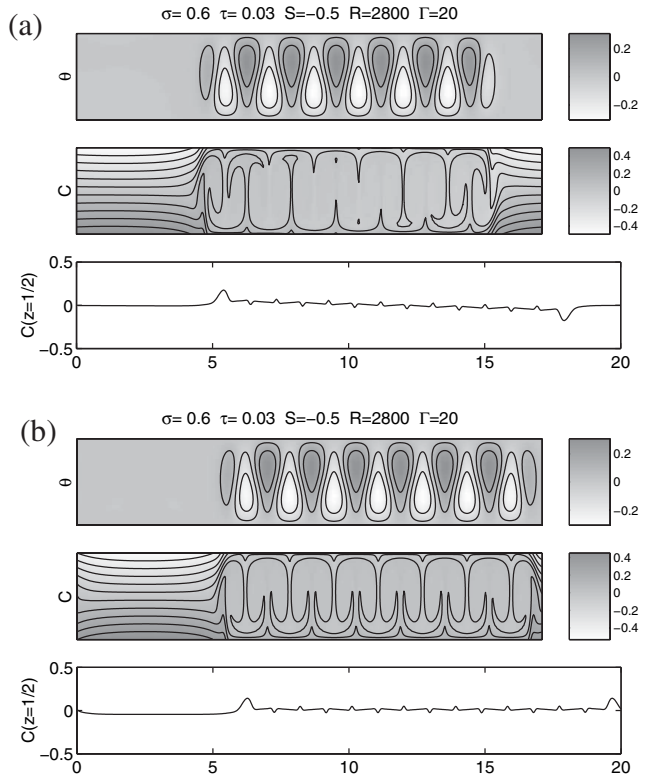

FIG. 1. (a) Odd and (b) even parity convectons at $R = 2800$ ($\epsilon = 0.1681$) in a ^{3}He-^{4}He mixture with $S = -0.5$, $\sigma = 0.6$, $\tau = 0.03$ and spatial period $\Gamma = 20$, in terms of contours of constant θ, C and midplane concentration $C(x, z = 1/2)$.

top and bottom boundaries. The resulting steplike profile in $C(x, z = 1/2)$ [Fig. 1(a)] is typical of this type of expulsion process [15], with dips in $C(x, z = 1/2)$ associated with downflow, and bumps with upflow. The inhomogeneity in the roll amplitude at the boundary of the convecton amplifies this effect and produces larger concentration anomalies at its edges; these anomalies in turn "trap" the convecton, much as discussed by Riecke in the context of self-trapping of wave packets [16]. We may think of these anomalies as the location of the bounding fronts. In contrast, the temperature boundary layers are substantially weaker, as expected in a system with $\tau \ll 1$, and do not contribute to self-trapping. Note that despite the fact that it is not left-right symmetric the odd convecton is in fact *stationary*. This is a consequence of the fact that it is symmetric [17] under the reflection $\rho = \rho_z \rho_x$, where ρ_x:$(x, z) \to (-x, z)$, $(u, w, \theta, \Sigma) \to (-u, w, \theta, \Sigma)$ with respect to a suitable origin, *and* ρ_z:$(x, z) \to (x, 1 - z)$, $(u, w, \theta, \Sigma) \to (u, -w, -\theta, -\Sigma)$. Evidently, if the fixed temperature boundary condition at the top (or the bottom) were changed into a Newton's law of cooling the odd parity convecton would drift at a constant speed, while the even one would remain at rest.

Figure 2(a) shows the evolution of a small amplitude initial perturbation into a convecton in the form of a space-time plot when $R = 2800$, $\Gamma = 30$ with time increasing upwards in units of the thermal diffusion time in the vertical. The waves grow as the initial perturbation disperses, leaving behind a void. This void "pushes" the remaining rolls into an incipient convecton and compresses the rolls within it. In the stationary state the convecton consists of stationary rolls of uniform amplitude, except for two "front"-like structures at either end that separate it from the void. Figure 3 shows the final state.

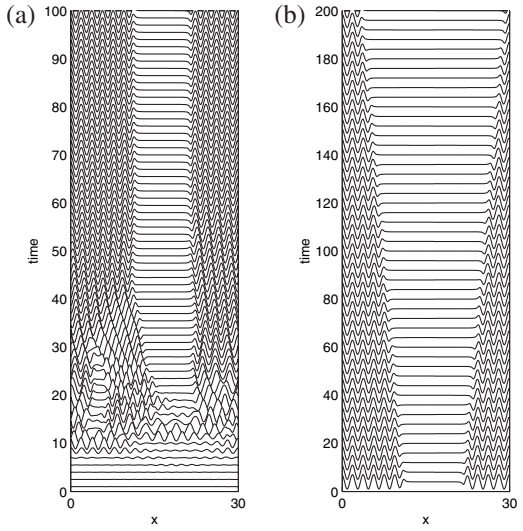

FIG. 2. (a) The formation of an odd parity convecton when $R = 2800$, $\Gamma = 30$ starting from small amplitude initial conditions, in the form of a space-time plot of $\theta(x, z = 1/2, t)$ with time increasing upward. (b) The destruction of this state when R is decreased from $R = 2800$ to $R = 2700$. Both fronts recede at the same rate preserving the parity of the state.

As R increases we find that the number of rolls within the convecton gradually increases. The transitions leading to the addition of a roll are hysteretic. However, once R reaches $R = 2900$ the behavior changes dramatically, with the void region now filled with traveling waves (Fig. 4). These propagate outward from the void center, growing in amplitude as they travel, and are responsible for the irregular oscillations of the interface between the convecton and void; these are in turn responsible for the fluctuations in the

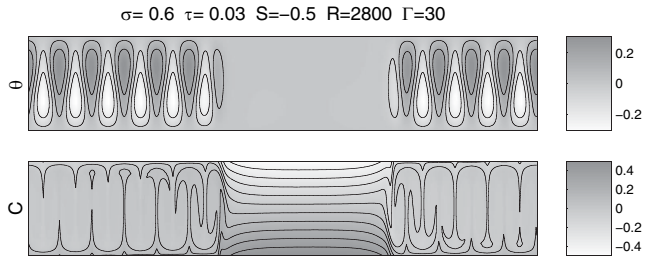

FIG. 3. An odd parity convecton formed in the process shown in Fig. 2(a); the convecton contains a larger number of rolls than the one shown in Fig. 1(a).

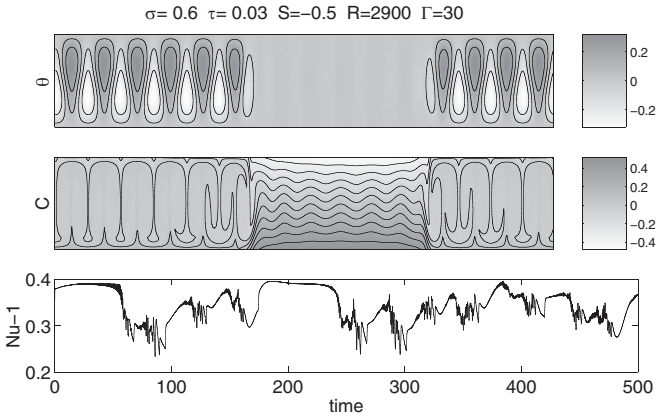

FIG. 4. Confined convectonlike state maintained by traveling waves in the void region when $R = 2900$, $\Gamma = 30$, and $t = 500$. The third panel shows the fluctuations in the Nusselt number arising from fluctuations in the number of rolls in the structure.

number of rolls in the convecton, as seen in the dimensionless convective heat flux $\mathrm{Nu}(t) - 1$, where Nu is the Nusselt number (Fig. 4).

In contrast, when R is decreased the number of rolls within the convecton gradually decreases. Figure 5 shows the associated decrease in the Nusselt number when R is reduced from $R = 2800$ to (a) $R = 2750$ and (b) $R = 2700$. In Fig. 5(a) the convecton simply becomes more compact while in Fig. 5(b) each of the barely visible oscillations in $\mathrm{Nu}(t)$ corresponds to the expulsion of a pair of rolls. If R is sufficiently small that a convecton consisting of two rolls is unstable this process leads to the destruction of the convecton [Fig. 2(b)]. Figure 5(b) shows that in this case the roll amplitude falls to a small value before a *new* convecton regrows as in Fig. 2(a). The convectons created in this nucleation process may have different numbers of rolls [Fig. 5(b)].

Localized steady states consisting of a finite number of roll-like structures generally occur as a consequence of spatial locking of the fronts bounding the state and the periodic structure within the state [18]. In this picture the localized states are associated with homoclinic connections to the homogeneous state. For bistable variational systems with reflection symmetry in one spatial dimension the process generating such states is well understood [19]: the states exist in a finite parameter interval spanning the Maxwell point, and are described by a pair of intertwined curves of homoclinics (one for odd states, the other for even states) that oscillate back and forth as they approach a spatially periodic roll state; with each turn the localized state acquires a pair of additional ''rolls.'' Thus there is a parameter interval with an infinite number of coexisting localized states of both parities; these appear in a sequence of saddle-node bifurcations involving stable and unstable solutions. States of this type have been seen in the Swift-Hohenberg equation with both quadratic and cubic terms [20]. Moreover, when the bifurcation parameter ϵ is reduced below the lowest value at which a stationary front is present the uniform state invades the structured state in ''jumps'' of one wavelength of the structure. Each of the resulting states can in principle be restabilized by increasing ϵ again. This picture extends to nonvariational systems,

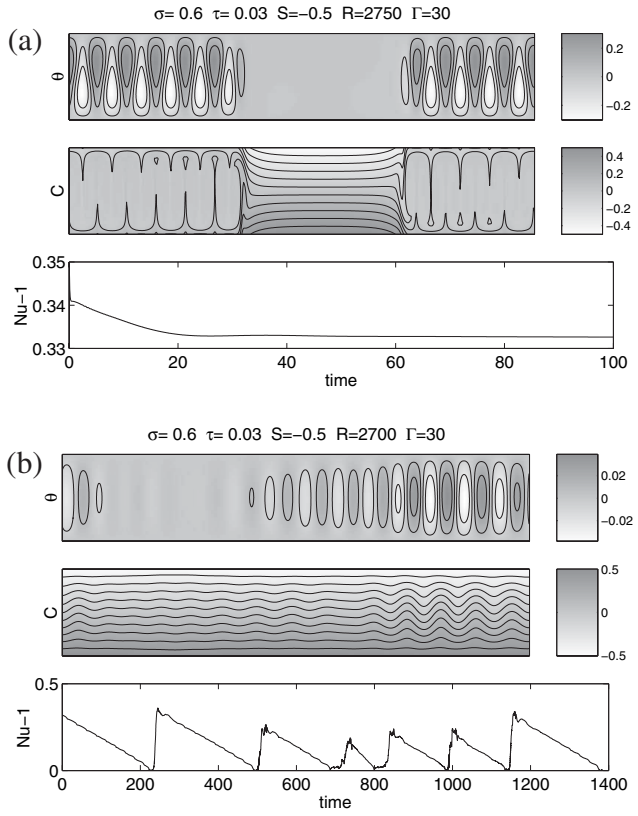

FIG. 5. The evolution of the odd parity convecton in Fig. 3 when R is decreased from $R = 2800$ to (a) $R = 2750$, (b) $R = 2700$, for $\Gamma = 30$. The top panels show the state at the final instant; the lower panels show the evolution of the Nusselt number, for comparison with Fig. 2(b).

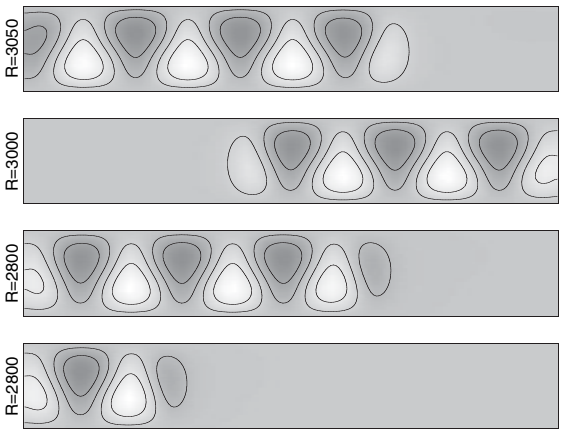

FIG. 6. A multiplicity of stable convectons in a bounded container of aspect ratio $\Gamma = 10$. The corresponding value of R is indicated at the left of each panel.

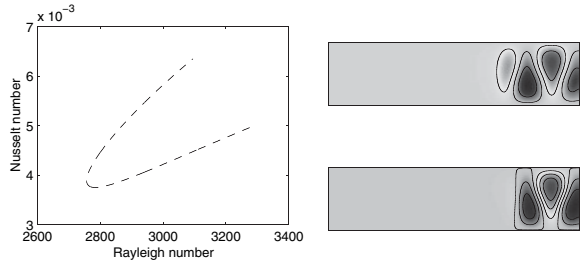

FIG. 7. A bifurcation diagram for convectons in a bounded container of aspect ratio $\Gamma = 10$. The panels on the right show the structure of the convecton in terms of θ at the two ends of the branch. The upper convecton is stable between the turning point and $R \approx 2800$; the lower is unstable.

like binary fluid convection, as well [21], and indeed the space-time plots in Fig. 2 resemble those computed in [21].

The above theory, however, applies only when the homogeneous and periodic states are both stable. We believe that the existence of convectons when $R > R_c$ is a consequence of two additional physical mechanisms. The expulsion of concentration gradients increases locally the value of ϵ by depressing R_c, while in the void regions the concentration difference between the bottom and top is unchanged. In these regions $\epsilon > 0$ but no instability occurs because the convectons serve as absorbing boundaries. These raise the instability threshold sufficiently to stabilize the conduction state in the void: $0 < \epsilon < \epsilon_c^{\text{void}}$. For example, the void associated with the convecton in Fig. 3 is of length $\Gamma^{\text{void}} \approx 10$; the critical Rayleigh number for the void with no-flux no-slip lateral boundary conditions is then $R_c^{\text{void}} \approx 2643$ and this number can be increased by reducing the effective reflection coefficient at the lateral boundaries [22]. We believe therefore that the void regions correspond to a locally absolutely stable conduction state; once $R > R_c^{\text{void}}$ the void fills with traveling waves (Fig. 4), much as observed in water-ethanol mixtures [8]. It is possible, however, that in experiments the voids may fill with waves even when $\epsilon < \epsilon_c^{\text{void}}$ [7,23]; such waves would have to be noise sustained [7,23] and would differ considerably from the waves in Fig. 4 [24].

Since the convectons are steady states of the system it comes as no surprise that they are also found in finite domains (Fig. 6), provided Γ is taken sufficiently large. In Fig. 7 we show the result of following a branch of such convectons as a function of R; the turn in the branch may be related to the oscillations in the branch of homoclinics predicted by the theory [19,21].

With recent improvements in visualization at cryogenic temperatures [25] the convecton states found here should be observable in experiments. Similar states are expected in water-ethanol mixtures as well.

This work was supported in part by the National Science Foundation under Grant No. DMS-0305968 and by DGICYT under Grant No. BMF2003-00657. We are grateful to A. Champneys for a very helpful discussion.

[1] T. S. Sullivan and G. Ahlers, Phys. Rev. A **38**, 3143 (1988); Phys. Rev. Lett. **61**, 78 (1988).
[2] P. Kolodner, C. M. Surko, and H. Williams, Physica (Amsterdam) **37D**, 319 (1989).
[3] V. Steinberg, J. Fineberg, E. Moses, and I. Rehberg, Physica (Amsterdam) **37D**, 359 (1989).
[4] P. Kolodner, Phys. Rev. E **47**, 1038 (1993).
[5] E. Moses, J. Fineberg, and V. Steinberg, Phys. Rev. A **35**, 2757 (1987); R. Heinrichs, G. Ahlers, and D. S. Cannell, Phys. Rev. A **35**, 2761 (1987).
[6] P. Kolodner, J. A. Glazier, and H. L. Williams, Phys. Rev. Lett. **65**, 1579 (1990); J. A. Glazier, P. Kolodner, and H. L. Williams, J. Stat. Phys. **64**, 945 (1991).
[7] P. Kolodner, S. Slimani, N. Aubry, and R. Lima, Physica (Amsterdam) **85D**, 165 (1995).
[8] P. Kolodner, Phys. Rev. E **48**, R665 (1993).
[9] S. Blanchflower, Phys. Lett. A **261**, 74 (1999).
[10] M. C. Cross, Physica (Amsterdam) **37D**, 315 (1989).
[11] O. Batiste and E. Knobloch, in *Perspectives and Problems in Nonlinear Science*, edited by E. Kaplan, J. Marsden, and K. Sreenivasan (Springer-Verlag, Berlin, 2003), pp. 91–144; Phys. Fluids **17**, 064102 (2005).
[12] G. Ahlers and I. Rehberg, Phys. Rev. Lett. **56**, 1373 (1986).
[13] T. J. Bloodworth, M. R. Ardron, J. K. Bhattacharjee, P. G. J. Lucas, and N. D. Stein, Nonlinearity **3**, 981 (1990).
[14] O. Batiste, M. Net, I. Mercader, and E. Knobloch, Phys. Rev. Lett. **86**, 2309 (2001); O. Batiste, E. Knobloch, I. Mercader, and M. Net, Phys. Rev. E **65**, 016303 (2002).
[15] E. Knobloch and W. J. Merryfield, Astrophys. J. **401**, 196 (1992).
[16] H. Riecke, Phys. Rev. Lett. **68**, 301 (1992); H. Riecke and W.-J. Rappel, Phys. Rev. Lett. **75**, 4035 (1995).
[17] E. Knobloch, Phys. Fluids **8**, 1446 (1996).
[18] Y. Pomeau, Physica (Amsterdam) **23D**, 3 (1986).
[19] G. W. Hunt, M. A. Peletier, A. R. Champneys, P. D. Woods, M. A. Wadee, C. J. Budd, and G. J. Lord, Nonlinear Dynamics **21**, 3 (2000), and references therein.
[20] M'F. Hilali, S. Métens, P. Borckmans, and G. Dewel, Phys. Rev. E **51**, 2046 (1995).
[21] P. Coullet, C. Riera, and C. Tresser, Phys. Rev. Lett. **84**, 3069 (2000); Prog. Theor. Phys. Suppl. **139**, 46 (2000).
[22] M. C. Cross, Phys. Rev. Lett. **57**, 2935 (1986).
[23] W. Schöpf and I. Rehberg, Europhys. Lett. **17**, 321 (1992).
[24] M. R. E. Proctor, S. M. Tobias, and E. Knobloch, Physica (Amsterdam) **145D**, 191 (2000).
[25] A. L. Woodcraft, P. G. J. Lucas, R. G. Matley, and W. Y. T. Wong, J. Low Temp. Phys. **114**, 109 (1999).